Synthesis of highly ordered mesoporous hybrid silica from aromatic fluorinated organosilane precursors†

Bénédicte Lebeau,*[a] Claire Marichal,[a] Alexia Mirjol,[b] Galo J. de A. A. Soler-Illia,[b] Ralf Buestrich,[c] Michael Popall,[c] Léo Mazerolles[d] and Clément Sanchez*[b]

[a] *Laboratoire de Matériaux Minéraux, CNRS UMR 7016, UHA, ENSCMu, 3 rue Alfred Werner, 68093, Mulhouse, France. E-mail: b.lebeau@univ-mulhouse.fr*
[b] *Laboratoire de Chimie de la Matière Condensée, CNRS UMR 7574, Université P. et M. Curie, 4 place Jussieu, 75252, Paris cedex 05, France. E-mail: clems@ccr.jussieu.fr*
[c] *Fraunhofer Institut für Silicatforshung, Würsburg, Germany*
[d] *Laboratoire Centre d'Etudes de Chimie Métallurgique (CECM), CNRS UPR 2801, 15 rue G. Urbain, 94407, Vitry sur Seine, France*

Received (in Montpellier, France) 11th July 2002, Accepted 16th September 2002
First published as an Advance Article on the web 10th December 2002

Organo-fluorinated mesoporous MCM-41 type silica presenting a high degree of order has been prepared from co-condensation of tetraethoxysilane (TEOS) and pentafluorophenyltriethoxysilane [PFPTES (**1**)] in the presence of cetyltrimethylammonium bromide as a template. Both basic and acidic routes have been explored. In the presence of an excess of water using fluoro-precursor (**1**), most of the bound fluoro-organic moieties are cleaved, yielding to pentafluorophenyl doped silica. Higher fluorine content silica-based MCM-41 materials were obtained by using 2-pentafluorophenylethyltriethoxysilane [PFPETES (**2**)] as the organosilane precursor. In that case, the fluoro-containing groups remain covalently bound to the mesoporous inorganic network, yielding materials with potential hydrophobic, adsorbing and optical properties.

Introduction

There is currently extensive effort to develop methods for the production of porous inorganic materials based on silica and other oxides because of their potential for wide practical applications (catalysis, photonics, chromatography, specific membranes, adsorbents, *etc.*). A key step in the synthesis of porous materials continues to be the use of supramolecular surfactant micellar or block copolymer templates for the inorganic framework, resulting in mesoporous M41S phases.[1] One goal in structural control has been to provide new accessible specific functions located in the internal pore surface. Chemical functionalisation of the inorganic framework of porous materials, for example through the covalent coupling of an organic moiety, is a promising approach to specific pore surface properties such as hydrophobicity, polarity, and catalytic, optical and electronic activity;[2–4] indeed, the tailoring of the pore surfaces presents direct interest in applications such as catalysis, chromatography, controlled delivery or membranes. Organo-functionalisation of ordered mesoporous silica-based solids can be achieved either by post-synthetic methods[5–9] or *via* direct routes (one-pot synthesis).[10–17] The latter involves co-condensation of tetraalkoxysilanes and organotrialkoxysilanes in the presence of surfactants. The one-pot synthesis method allows a higher organic content and a more homogeneous organic distribution in the material.[18] Numerous studies have pointed out the role and importance of the nature of the bonds comprising the hybrid inorganic–organic interface.[19] Hybrid materials with covalently bonded organic moieties (Class II hybrids[19]) can be readily designed by sol–gel chemistry and thus a wide range of materials with tailor-made structure and properties can be reproducibly prepared. However, to the best of our knowledge, practically no work has been reported on periodically organised mesoporous organo-fluorinated silicas. This is probably due to the difficulties in compatibilising the self assembly of the template, the inorganic and the fluorinated moieties, as well as the lack of fluoro-organosilane availability. The present research describes the first synthesis of ordered fluoro-organically modified mesoporous silica.

Fluoro-organically modified mesoporous silicas were first synthesized under basic or acidic conditions from co-condensation of tetraethoxysilane (TEOS) and pentafluorophenyltriethoxysilane (PFPTES, hereafter **1**) or 2-pentafluorophenylethyltriethoxysilane (PFPETES, hereafter **2**) in the presence of the surfactant cetyltrimethylammonium bromide (C_{16}TMABr). Final products were characterised by XRD, FTIR, chemical analysis, TGA–DTA, N_2 adsorption–desorption, ^{13}C, ^{19}F and ^{29}Si solid state MAS-NMR, and transmission electron microscopy (TEM).

Experimental

Synthesis of fluoro-organosilane precursors

Precursor **1** was synthesized by following the procedure described elsewhere[20] (Fig. 1a). 24.7 g (100 mmol) pentafluorobromobenzene (PFBB), 2.65 g (110 mmol) magnesium turnings, 41.70 g (200 mmol) freshly distilled TEOS and a few crystals of iodine were mixed together at room temperature and diethyl ether was added drop-wise to the vigorously stirred mixture until an exothermic reaction was observed (approx. 30 min). After stirring and refluxing for 16 h the mixture was cooled to room temperature. An excess of n-heptane was added to precipitate the magnesium salts. Filtration gave a

† Electronic supplementary information (ESI) available: detailed characterisation of sample C (TEOS/PFPETES 9/1). See http://www.rsc.org/suppdata/nj/b2/b206924p/

 DOI: 10.1039/b206924p

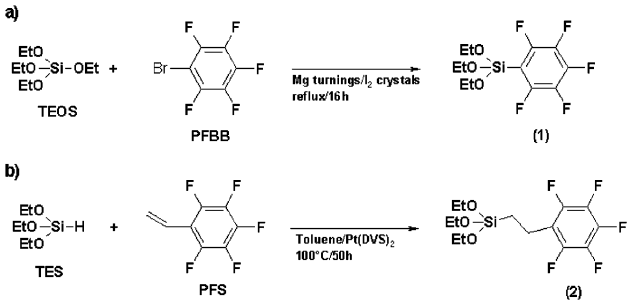

Fig. 1 Reaction schemes for a) PFPTES (**1**) and b) PFPETES (**2**) fluorinated precursors.

clear pale yellow solution. Solvents were removed and the residue fractionally distilled under reduced pressure (18 Torr). ^{1}H NMR ($CDCl_3$) δ: −1.28 (3H, OCH_2CH_3); −3.96 (2H, OCH_2CH_3). ^{19}F NMR ($CDCl_3$) δ: −127.2 (2F, *ortho*); −151.0 (1F, *para*); −161.9 (2F, *meta*).

Precursor **2** was synthesised by coupling a pentafluorostyrene (PFS) group to triethoxysilane (TES) *via* a hydrosilylation reaction (Fig. 1b). Platinum-1,3-divinyltetramethyldisiloxane (Pt(DVS), 0.24% Pt, solution in xylene, ABCR, Karlsruhe) was used as catalyst for the hydrosilylation reaction.[21] 56 mmol (9.19 g) of TES in 20 ml of dry toluene were introduced first into a three-necked round-bottomed flask under argon atmosphere and cooled to 0 °C with an ice bath. 56 mmol (10.88 g) of PFS in 20 ml of dry toluene were added under stirring to the TES solution. 0.784 mmol (350 µl) of Pt(DVS) was then added under stirring and the resulting mixture was heated at reflux (110 °C) for 50 h. Most of the platinum colloids were removed by centrifugation (20 000 rpm for 20 min). Toluene was then removed by evaporation under vacuum; this operation was repeated to ensure complete elimination of volatile unreacted starting products (checked by NMR). A transparent yellowish liquid was finally obtained. ^{1}H NMR ($CDCl_3$) δ: 0.9 (t, $(CH_3CH_2O)_3Si$–CH_2CH_2–C_6F_5); 1.2 (t, CH_3CH_2O); 2.7 (t, $(CH_3CH_2O)_3Si$–CH_2CH_2–C_6F_5); 3.85 (q, CH_3CH_2O). ^{19}F NMR ($CDCl_3$) δ: −148.4 (2F, *ortho*), −160.7 (1F, *para*); −165.0 (2F, *meta*).

Preparation of fluorine-containing mesoporous silica solids

The samples were synthesized from either an alkaline or an acidic mixture containing one of the following molar compositions: 0.12 C_{16}TMABr:0.50 NaOH:1 − x TEOS:x **1** (or **2**):130 H_2O or 0.12 C_{16}TMABr:9.2 HCl:1 − x TEOS:x **1**:130 H_2O (x = 0.1 or 0.2). In a typical preparation under alkaline conditions, 0.80 g of C_{16}TMABr (Aldrich) was dissolved in 42.8 ml of 0.1 M NaOH. The appropriate amounts of TEOS (Aldrich) and **1** (or **2**) were added, and the mixture was stirred for 24 h at room temperature. The solid product was filtered, washed with H_2O and dried for 24 h in an oven at 60 °C. Extraction of the surfactant was performed by stirring a suspension of the solid product (1 g) in 1.0 mol dm^{-3} HCl in EtOH (25 ml of HCl 37% (Prolabo) mixed with 300 ml of absolute EtOH) at 70 °C for 24 h. The surfactant-extracted material was filtered, washed with EtOH and dried for 24 h at 60 °C. For preparations under acidic conditions, the same general preparation was used, except that the 0.1 M NaOH aqueous solution was replaced by a 3.85 M HCl aqueous solution. The synthetic details of the different samples prepared are summarised in Table 1.

Characterisation

Nuclear magnetic resonance (NMR). ^{1}H and ^{19}F NMR spectra of fluoro-organosilane precursors **1** and **2** were obtained in $CDCl_3$ as solvent using a Bruker WM 400 and a Bruker AC 250, respectively. Solid state NMR experiments were run on an MSL300 (^{13}C at 75.4 MHz and ^{29}Si at 59.6 MHz) and DSX400 (^{19}F at 376.5 MHz) Bruker spectrometers. Samples were introduced into a 4 mm or 2.5 mm spinner and spun at 4 kHz (for ^{13}C and ^{29}Si NMR acquisitions), 8 kHz and 15 kHz (for ^{19}F NMR acquisitions). MAS ^{29}Si NMR experiments were made by using a 2 µs pulse ($\pi/6$) with a recycle delay of 60 s. CP-MAS ^{13}C NMR experiments were run with a contact time of 1 ms and a recycle delay of 10 s. MAS ^{19}F NMR spectra were recorded with a 5.5 µs pulse ($\pi/2$) and a recycle delay of 60 s. Tetramethylsilane was used as external chemical shift reference for ^{1}H, ^{13}C and ^{29}Si NMR experiments. $CFCl_3$ was used as external chemical shift reference for ^{19}F NMR experiments.

Table 1 Synthetic conditions for the fluorine-containing mesoporous silica solids

Sample identification	Organosilane precursor	x^a	Catalyst
A1	**1**	0.1	NaOH
A2	**1**	0.2	NaOH
B1	**1**	0.1	HCl
B2	**1**	0.2	HCl
C	**2**	0.1	NaOH

[a] Initial organosilane molar content.

X-Ray diffraction (XRD). XRD patterns were recorded on a powder PW 1130 Philips diffractometer using Cu Kα radiation (λ = 1.5406 Å).

Porosimetry. N_2 adsorption–desorption measurements were performed on an ASAP 2010 Micromeritics equipment.

Fourier transform infra-red (FTIR). FTIR transmission spectra were recorded on pressed KBr pellets on a Nicolet Magna-IR 550 spectrophotometer.

Chemical analyses. Fluorine loadings in final products were measured using elemental analysis at the Service Central des Analyses, CNRS, Vernaison, France.

Transmission electron microscopy (TEM). TEM observations were made using a TOPCON 002B microscope operating at 200 kV. Samples were observed either directly after deposition of powder on a copper grid or as ultramicrotomed slices after embedding in an epoxy resin.

Results and discussion

Ordered mesoporous silica modified with PFPTES (precursor 1)

XRD patterns obtained from surfactant-extracted samples prepared under alkaline conditions (A1 and A2) showed four broad Bragg reflections that can be indexed as d_{100}, d_{110}, d_{200} and d_{210} (see Fig. 2 and Table 2) and are characteristic of a hexagonal symmetry. The presence of these four diffraction peaks indicated that both samples A1 and A2 have MCM-41 type architecture with long range order. Two broader Bragg reflections were observed on the XRD pattern of sample B2, which can be indexed as d_{100} and d_{110}. These two diffraction peaks are consistent with a hexagonal symmetry but with a low degree of organisation. Concerning sample B1, the XRD pattern displayed only one broad Bragg diffraction that indicates a disordered worm-like mesostructure, as in the case of HMS materials.[22]

Acidic conditions lead to less ordered mesostructured silica materials than alkaline conditions. Three main processes, which are known to be different in acid or alkaline media, can be held responsible for such observed differences: a) the

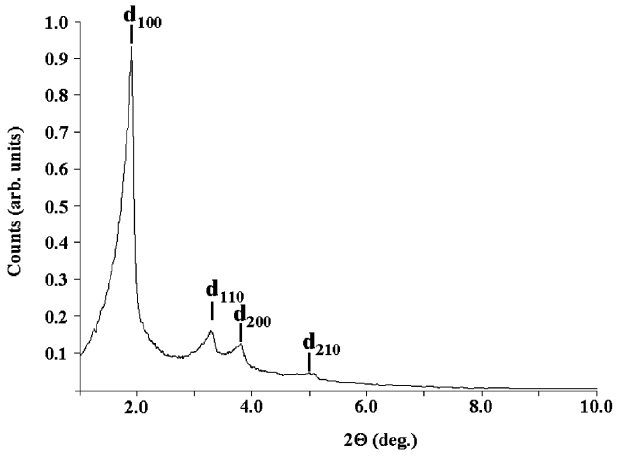

Fig. 2 XRD pattern of the surfactant extracted sample A2.

nature of the surfactant (S)/inorganic (I) interfaces,[23] b) the kinetics of hydrolysis/co-condensation of TEOS and the fluorinated precursors,[24] c) the kinetics of the cleavage of the organofluoro-moieties (*vide infra*). An electrostatic I^-S^+ synthetic path was identified for the basic route whereas an electrostatic $I^+X^-S^+$ synthetic path (X = Cl) was identified for the acid route. In the latter case, the interaction I/S is more "fuzzy", which should lead to a less ordered mesostructure. Indeed, it has been observed that basic synthesis conditions lead to better ordered organosilicas.[25] High ionic strength is also probably responsible for the improved organisation of surfactant aggregates and, thus, for the high degree of organisation of the hybrid mesostructured complex that forms in the basic medium. Values of d_{100}-spacing obtained from XRD patterns are higher for samples prepared under alkaline conditions (48.8 and 46.5 Å) than for samples made under acidic conditions (32.0 and 35.2 Å). Such differences may be explained by a higher wall thickness for the samples obtained from basic solutions (A1 and A2 samples, *vide infra*), a consequence of the higher condensation degree reached in alkaline media. TEM images of the A2 material (alkaline conditions) showed hexagonal sets of lattice fringes, as well as parallel fringes corresponding to side-on projections of the mesostructure (Fig. 3), which are consistent with the long range order parameters determined by XRD.

Type-IV N_2 adsorption–desorption isotherms characteristic of mesoporous solids were obtained for all surfactant-free samples. BET specific surface areas (S_{BET}) and average BJH pore diameters ($Ø_{BJH}$) are reported in Table 2. For samples A1 and A2 a sharp condensation capillary step was observed (Fig. 4) that indicates a small pore size distribution. Whatever the catalyst used, the S_{BET} values are high and similar. Slightly higher S_{BET} values were measured for high initial F/Si molar ratio (about 1050 $m^2\ g^{-1}$) than for low initial F/Si molar ratio (about 950 $m^2\ g^{-1}$). Samples prepared under alkaline conditions present higher average pore diameters (28.8 and 29.5 Å) than samples made under acidic conditions (22.7 and 22.2 Å). Taking into account the XRD data, the materials prepared *via* the basic route present a wall thickness of about 20 Å, compared with about 10 Å for the materials prepared from an acidic route. From these results, it seems that both wall thickness and pore diameter explain the higher *d*-spacings observed for samples made from a basic route. Micelle size (and therefore, the cavity size) should also be related to the characteristics of the medium (pH, ionic force, counterions, *etc.*).[25]

FTIR spectra recorded on as-synthesised samples showed clearly three groups of bands: shoulders at 1410–1450 cm^{-1}, a doublet at 1506–1523 cm^{-1} and a broad band at 1620–1650 cm^{-1}; all these bands are characteristic of aromatic $\nu_{C=C}$ ring vibration and aromatic C=C stretching bands, respectively. C–F stretching frequencies (bands at 1076, 1131 and 1152 cm^{-1}) are overlapped by the Si–O stretching modes (950–1200 cm^{-1}).[26] Vibrations indicative of the surfactant at 2850–2950 cm^{-1} were also observed. However, the bands due to C=C bonds as well as the bands characteristic of the surfactant were not detectable in the spectra of the surfactant-extracted samples. A ^{13}C MAS NMR study confirmed the absence of pentafluorophenyl groups and surfactant molecules in the final materials.

F/Si molar ratios in final materials, calculated from chemical analyses, are reported in Table 2. In all cases final F/Si molar ratios are much lower than initial F/Si molar ratios and indicate the incorporation of 0.6 and about 8% of fluorinated groups for surfactant-extracted materials made under acidic and basic conditions, respectively. Final F/Si molar ratios of 0.02 and 0.1 were measured in as-synthesised high nominal fluorine ratio samples B2 and A2, respectively. These results indicate that a great part of the fluorine component has been lost during the formation of the first hybrid mesophase.

Three resonance lines at −129.6, −150.7 and −164.7 ppm were observed in the ^{19}F MAS NMR spectrum of the as-synthesised high fluorine content sample made from a basic mixture (Fig. 5). These resonances correspond to the three types of fluorine nuclei from the pentafluorophenyl groups in *ortho*, *para* and *meta* positions, respectively. After surfactant extraction only the peak at −129.6 ppm is clearly observed in the ^{19}F MAS NMR spectrum. Resonances of fluorine nuclei from the pentafluorophenyl group are not clearly observed in the ^{19}F MAS NMR spectra of the as-synthesised and surfactant-extracted high fluorine content samples made from acidic mixtures. The fluorine content of these latter materials is probably too low to be detectable by ^{19}F MAS NMR spectroscopy. These results are in agreement with the chemical analysis data and confirmed by ^{29}Si MAS NMR experiments.

For all samples, the collected spectra displayed three resonances at about −92, −101 and −110 ppm that correspond to Q_2, Q_3 and Q_4 units, respectively (Fig. 6). In all cases the resonances characteristic of Q_3 and Q_4 are predominant

Table 2 XRD [*d*-spacings and unit cell parameter ($a = 2d_{100}/\sqrt{3}$)], N_2 adsorption–desorption [BET specific surface area (S_{BET})] and adsorption BJH pore diameter ($Ø_{BJH}$) and chemical analysis data [F/Si initial (F/Si_i)[a] and final (F/Si_f) molar ratios] of surfactant extracted fluorine-containing mesoporous silica solids

	XRD *d*-spacings and *a*/Å					N_2 adsorption–desorption		Chemical analysis	
Sample	d_{100}	d_{110}	d_{200}	d_{210}	*a*	$S_{BET}/m^2\ g^{-1}$	$Ø_{BJH}$/Å	F/Si_i[a]	F/Si_f
A1	48.8	28.1	24.4	18.8	56.3	940	28.8	0.5	0.021
A2	46.5	26.8	23.2	17.6	53.7	1060	29.5	1.0	0.077
B1	32.0	—	—	—	37.0	960	22.7	0.5	0.003
B2	35.2	20.3	—	—	40.6	1020	22.2	1.0	0.006
C	37.1	21.8	18.7	14.2	43.3	1260	27.0	0.5	0.300

[a] Initial F/Si molar ratio was determined from the experimental conditions.

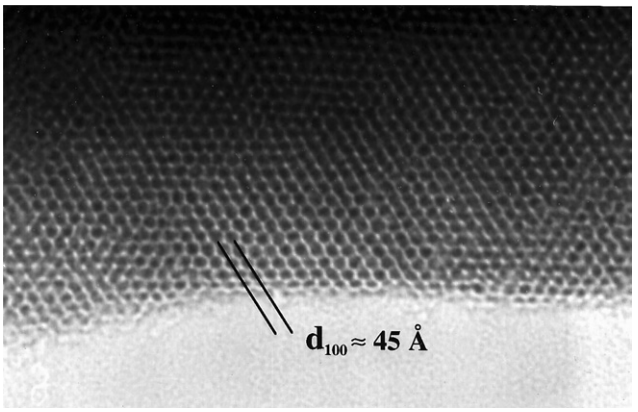

Fig. 3 TEM micrograph of the surfactant-extracted sample A2.

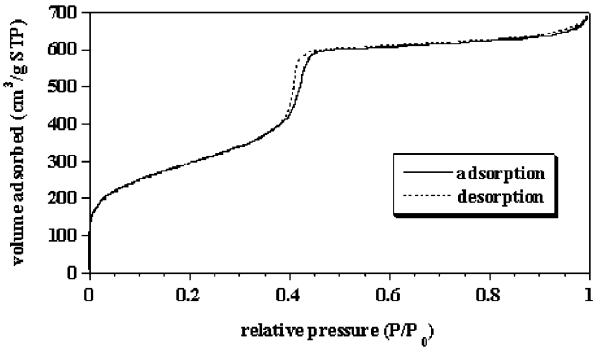

Fig. 4 N_2 adsorption–desorption isotherm of the surfactant extracted sample A2.

(>95%) and the Q_4 peak is more intense (>60%). These results are in agreement with extensive condensation of the silica walls. A condensation degree of about 90% was calculated. No T units corresponding to species issued from **1** could be clearly observed. The disappearance of most of the fluorine is due to the cleavage of the Si–C_{sp^2} bond. Such cleavage might be activated by the attractor inductive effect of fluorine atoms.[27] This phenomenon occurs mainly during the material formation and the surfactant extraction process, and appears to be favoured by the presence of acid.

Ordered mesoporous silica modified with 2-pentafluorophenylethyltriethoxysilane [PFPETES (*2*)]

The XRD patterns recorded for sample C (functionalised with precursor **2**) before and after surfactant extraction show four diffraction peaks in the 2θ range 1–10° that can be indexed as d_{100}, d_{110}, d_{200} and d_{210} and indicate a 2D-hexagonal symmetry (see Table 2 and ESI).‡ Sample C exhibits a MCM-41-type architecture with a unit cell parameter a of 43.3 Å. High resolution TEM imaging showed the presence of highly ordered single domain 'crystals' of MCM-41 silica with a hexagonal lattice parameter from the Fourier transform filtered image of $a = 34.6$ Å ($d_{100} = 30$ Å) (Fig. 7). The difference between the d-values obtained by XRD and TEM can be attributed to shrinking of the inorganic network during the imaging process; in fact, the C samples are unstable under the electron beam, due to the appreciable quantity of organic material.

‡ Acidic media have also been used to obtain mesostructured silica functionalised by precursor **2**. Under the explored conditions, only a worm-like ordering has been obtained, similar to those samples modified by **1**. These poorly organised solids are not further discussed in this paper.

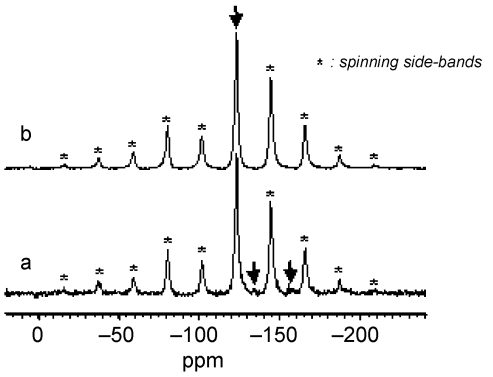

Fig. 5 ^{19}F MAS NMR spectrum of the as-synthesized (a) and surfactant extracted (b) sample A2.

Type-IV isotherms are obtained by N_2 adsorption–desorption measurements, which are characteristic of a high surface area mesoporous solid (1260 $m^2\ g^{-1}$, see ESI). A sharp pore size distribution was observed with an average BJH pore diameter of 27 Å. Taking into account the d_{100} value measured by XRD, the pore wall thickness is about 10 Å.

The FTIR spectra of as-synthesised samples C (Fig. 8) clearly showed the same $\nu_{C=C}$ vibration bands present in the A and B samples (groups at 1410–1456, 1490–1530 and 1620–1650 cm^{-1}). In addition, two ν_{C-F} vibration bands are clearly observed in the as-synthesised spectrum (1120 and 1154 cm^{-1}). Surfactant bands (ν_{C-H} bands at 2850–2950 cm^{-1} and δ_{C-H} *ca.* 1470 cm^{-1} from C_{16}TMABr) are also observed. The latter are absent in the extracted material. Moreover, the aromatic and C–F bands characteristic of the fluoroaryl dangling groups are conserved in the extracted material, demonstrating that the extraction is efficient at completely removing the surfactant without damaging the grafted functions. This is confirmed by TGA–DTA measurements performed on as-synthesised and surfactant-extracted samples (see ESI). TGA curves show a 53% mass loss before 400 °C, which can be attributed to the elimination of the C_{16}TMABr.[28] A minor mass loss of 6% between 420 and 550 °C is also observed. Extracted samples display a mass loss of *ca.* 17% in this range, which coincides with an exothermic DTA peak centred at 480 °C. This decomposition step can be ascribed to the fluoro-organic functions. Indeed, the TG mass loss in this step is in agreement with the detected fluorine contents for extracted C samples (5–6% Si–F/Si_{total}, *i.e.* F/Si ≈ 0.25–0.3), confirming the higher incorporation of the fluoro-organic group, and the absence of significant leaching of the organic functions upon extraction.

The ^{19}F MAS NMR spectrum of the surfactant-extracted sample C exhibited three lines at −148.6, −164.9 and −168.2 ppm that can be attributed to the aromatic fluorine nuclei in

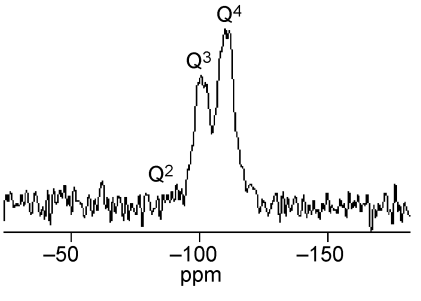

Fig. 6 ^{29}Si MAS NMR spectrum of the surfactant-extracted sample A2.

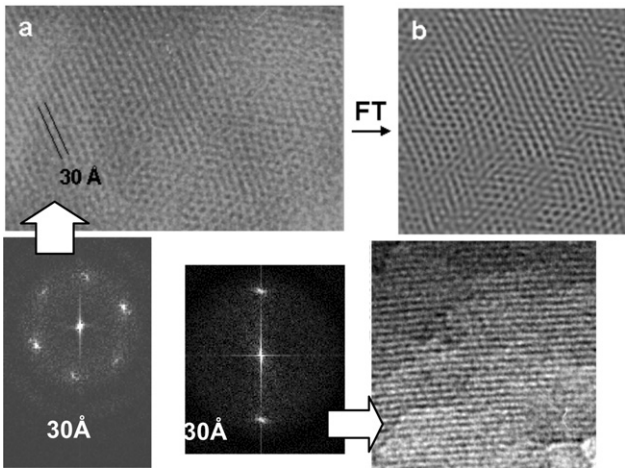

Fig. 7 TEM micrographs of sample C (a) and the Fourier transform (FT) filtered image (b). The presence of channels (c) confirms a 2D hexagonal mesostructure. Repeating distances of 30 Å are calculated from the Fourier transforms of the image.

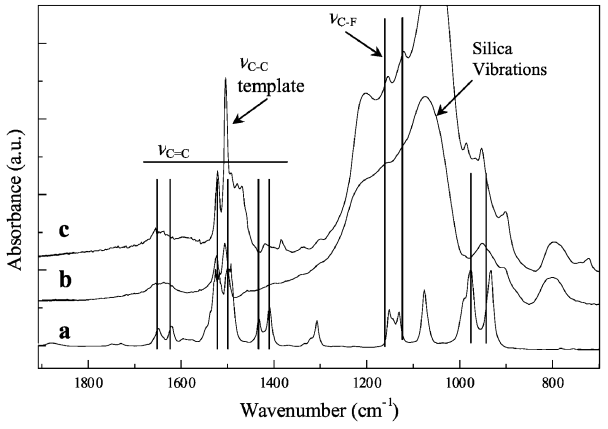

Fig. 8 FTIR spectra of a) pentafluorostyrene (PFS), b) sample C as-prepared, c) sample C, extracted with acidic ethanol. Relevant C=C and C–F vibrations are indicated.

ortho, *para* and *meta* positions (Fig. 9). A much less intense line was also observed at −175.5 ppm and was attributed to the presence of an impurity. The ^{13}C MAS NMR data confirm the presence of aromatic carbons at 116.6, 136.5, 139.3, 144.1 and 146.8 ppm. The line at 116.6 ppm was assigned to the quaternary carbon bonded to the ethyl spacer. From a spectral simulation of **2** with ACD-Lab Software, the lines at 136.5, 139.3 and 144.1 were attributed to carbons in *meta*-, *ortho*- and *para*-positions, respectively. Two weak and unresolved

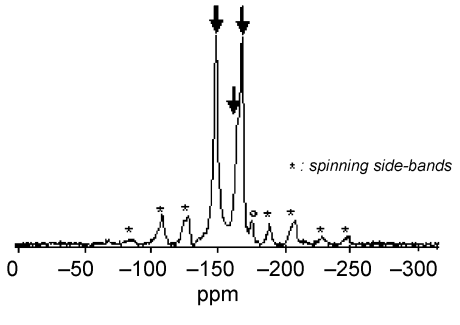

Fig. 9 ^{19}F MAS NMR spectrum of the surfactant-extracted sample C.

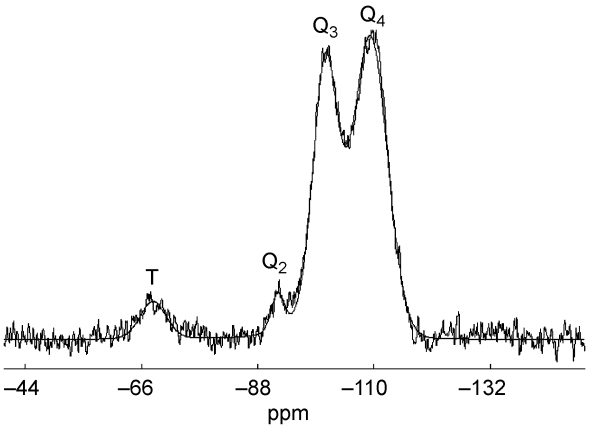

Fig. 10 ^{29}Si MAS NMR spectrum of the surfactant-extracted sample C; the smooth line corresponds to the simulated spectrum.

signals at 12.1 and 27.4 ppm were present and were assigned to CH_2–CH_2–Si and CH_2–CH_2–Si of the ethyl spacer, respectively. Two sharp lines were also observed at 16.1 and 58.5 ppm that can be assigned to the CH_3 and CH_2 of residual ethoxy groups, respectively. ^{29}Si MAS NMR spectroscopy showed distinct resonances for siloxane ($Q^n = Si(OSi)_n(OH)_{4-n}$, $n = 2$–4) and organosiloxane ($T^m = RSi(OSi)_m(OH)_{3-m}$, $m = 1$–3) centres, from TEOS and precursor **2**, in the surfactant-extracted material C (Fig. 10). A T/Q molar ratio of 6/94 and a condensation degree of 84% for the siloxane network were calculated from the fit of the spectrum with WINFIT software.[29] The presence of residual ethoxy groups reveals incomplete hydrolysis and condensation of precursor **2** which may explain the lower T/Q ratio in the surfactant-extracted material compared to the initial T/Q molar ratio of 10/90. However, this synthetic procedure allows grafting of higher fluorophenyl contents than the precursor route starting from precursor **1**.

Conclusion

Highly ordered fluorine-containing mesoporous siliceous materials with MCM-41-type architecture were prepared for the first time from co-condensation of TEOS and a fluoro-organic precursor (**1** or **2**). For materials obtained using precursor **1**, the Si–C_{sp^2} bonds were cleaved during the formation and the surfactant extraction processes, leading to fluorine-doped (*i.e.* F/Si < 0.06) MCM-41 silica materials. However, a better choice of fluoro-organosilane (precursor **2**) containing an alkyl spacer between the pentafluorophenyl group and the silicon centre allows one to preserve the organic functionality, leading to ordered mesoporous MCM-41-type siliceous materials with higher fluorine contents (F/Si ≈ 0.3).

Further investigations are in due course to improve the fluorine loading, to evaluate the hydrophobic and fluorophilic character of such materials for separation and adsorption applications, and to shape these materials as transparent thin films for optical devices.

Acknowledgements

The authors are grateful for funding from CNRS and Fundación Antorchas; AM acknowledges participation in a student project from ESCOM Cergy-Pontoise. GJAASI is a member of CONICET.

References

1 (*a*) J. S. Beck, J. C. Vartuli, W. J. Roth, M. E. Leonowicz, C. T. Kresge, K. D. Schmitt, C. T.-W. Chu, D. H. Olson, E. W. Sheppard, S. B. McCullen, J. B. Higgins and J. L. Schlenker, *J. Am. Chem. Soc.*, 1992, **114**, 10 834. Recent reviews include J. Y. Ying, C. Mehnert and M. S. Wong, *Angew. Chem., Int. Ed.*, 1999, **38**, 57; (*c*) T. J. Barton, L. M. Bull, W. G. Klemperer, D. A. Loy, B. McEnaney, M. Misono, P. A. Monson, G. Pez, G. W. Scherer, J. C. Vartuli and O. M. Yaghi, *Chem. Mater.*, 1999, **11**, 2633; (*d*) G. J. A. A. Soler-Illia, C. Sanchez, B. Lebeau and J. Patarin, *Chem. Rev.*, 2002, **102**, 4093.

2 K. Moller and T. Bein, *Chem. Mater.*, 1998, **10**, 2950.

3 A. Stein, B. J. Melde and R. C. Schroden, *Adv. Mater.*, 2000, **12**, 1403–1419.

4 A. Sayari and S. Hamoudi, *Chem. Mater.*, 2001, **13**, 3151.

5 R. Burch, N. Cruise, D. Gleeson and S. C. Tsang, *Chem. Commun.*, 1996, 951.

6 T. Maschmeyer, F. Rey, G. Sankar and J. M. Thomas, *Nature*, 1995, **378**, 159.

7 D. Brunel, A. Cauvel, F. Fajula and F. DiRenzo, *Stud. Surf. Sci. Catal.*, 1995, **97**, 173.

8 D. Brunel, *Microporous Mesoporous Mater.*, 1999, **27**, 329.

9 D. Brunel, A. C. Blanc, A. Galarneau and F. Fajula, *Catal. Today*, 2002, **73**, 139.

10 S. L. Burkett, S. D. Sims and S. Mann, *Chem. Commun.*, 1996, 1367.

11 C. E. Fowler, S. L. Burkett and S. Mann, *Chem. Commun.*, 1997, 1769.

12 D. J. MacQuarrie, *Chem. Commun.*, 1996, 1961.

13 M. H. Lim, C. F. Blanford and A. Stein, *J. Am. Chem. Soc.*, 1997, **119**, 4090.

14 F. Babonneau, L. Leite and S. Fontlupt, *J. Mater. Chem.*, 1999, **9**, 175.

15 L. Mercier and T. J. Pinnavaia, *Chem. Mater.*, 2000, **12**, 188.

16 Y. Lu, H. Fan, N. Doke, D. A. Loy, R. A. Assink, D. A. Lavan and C. J. Brinker, *J. Am. Chem. Soc.*, 2000, **122**, 5258.

17 (*a*) T. Asefa, M. J. Maclachlan, N. Coombs and G. A. Ozin, *Nature*, 1999, **402**, 867; (*b*) S. Inagaki, G. Shiyou, T. Ohsuna and O. Terasaki, *Nature*, 2002, **416**, 304; (*c*) B. J. Melde, B. T. Holland, C. F. Blanford and A. Stein, *Chem. Mater.*, 1999, **11**, 3302.

18 M. H. Lim and A. Stein, *Chem. Mater.*, 1999, **11**, 3285.

19 C. Sanchez and F. Ribot, *New J. Chem.*, 1994, **18**, 1007.

20 C. Roscher and M. Popall, *Mater. Res. Soc. Symp. Proc.*, 1996, **435**, 547.

21 C. Zhang, F. Babonneau, C. Bonhomme, R. M. Laine, C. L. Soles, H. A. Hristov and A. F. Yee, *J. Am. Chem. Soc.*, 1998, **120**, 8380.

22 S. A. Bagshaw, E. Prouzet and T. J. Pinnavaia, *Science*, 1995, **269**, 1242.

23 (*a*) Q. Huo, D. I. Margolese, U. Ciesla, P. Feng, Thurman E. Gier, P. Sieger, R. Leon, P. M. Petroff, F. Schüth and G. D. Stucky, *Nature*, 1994, **368**, 317; (*b*) Q. Huo, D. I. Margolese, U. Ciesla, D. K. Demuth, P. Feng, T. E. Gier, P. Sieger, A. Firouzi, B. F. Chmelka, F. Schüth and G. D. Stucky, *Chem. Mater.*, 1994, **6**, 1176.

24 H. Schmidt, H. Scholze and A. Kaiser, *J. Non-Cryst. Solids*, 1984, **63**, 1.

25 C. E. Fowler, PhD Thesis, University of Bristol, UK, 2001.

26 G. Socrates, *Infrared Characteristic Group Frequencies. Tables and charts*, Wiley, Chichester, 1994.

27 (*a*) C. Eaborn, I. D. Jenkins and D. R. M. Walton, *J. Chem. Soc., Perkin Trans. 2*, 1974, 596; (*b*) C. Eaborn and K. C. Pande, *J. Chem. Soc.*, 1960, 1566.

28 M. T. J. Keene, R. D. M. Gougeon, R. Denoyel, R. K. Harris, J. Rouquerol and P. L. Llewellyn, *J. Mater. Chem.*, 1999, **9**, 2843.

29 D. Massiot, F. Fayon, M. Capron, I. King, S. Le Calvé, B. Alonso, J.-O. Durand, B. Bujoli, Z. Gan and G. Hoatson, *Magn. Res. Chem.*, 2002, **40**, 70.